Search for intruder states in neutron rich nuclei ^{45,46}Ar

Zs. Dombrádi, D. Sohler, J. Timár, Z. Elekes

Institute of Nuclear Research, H-4001 Debrecen, Pf. 51, Hungary

O. Sorlin, F. Azaiez, F. Amorini,[1] M. Belleguic, C. Bourgeois, C. Donzaud, J. Duprat, D. Guillemaud-Mueller, F. Ibrahim, J. A. Scarpaci

Institut de Physique Nucléaire, IN2P3-CNRS, F-91406 Orsay Cedex, France

M. Stanoiu, M. J. Lopez, M. G. Saint-Laurent, F. Becker, M. Lewitowicz, F. Sarazin, C. Stodel, G. Voltolini

GANIL, B. P. 55027, F-14076 Caen Cedex 5, France

S. M. Lukyanov, V. Maslov, Yu.-E. Penionzhkevich

FLNR, JINR, 141980 Dubna, Moscow region, Russia

F. Nowacki

IReS, IN2P3-CNRS, Université Louis Pasteur, BP 28, F-67037 Strasbourg Cedex, France

G. Sletten

NBI, University of Copenhagen, Copenhagen, Denmark

R. Lucas, C. Theisen

CEA-Saclay, DAPNIA-SPhN, F-91191 Gif sur Yvette Cedex, France

D. Baiborodin, Z. Dlouhy, J. Mrazek

Nuclear Physics Institute, AS CR, CZ 25068, Rez, Czech Republic

C. Borcea

IFIN-HH, P. O. Box MG-6, 76900 Bucarest-Magurele, Rumania

A. Bauchet

CSNSM, IN2P3-CNRS and Université Paris-Sud, F-91405 Orsay Campus, France

C. Moore, M. Taylor

Oliver Lodge Laboratory, University of Liverpool, Liverpool L69 7ZE, U.K.

Abstract

The structure of the N≃28 $^{45,46}_{18}$Ar$_{27,28}$ nuclei has been investigated through in-beam γ-spectroscopy using the fragmentation reaction of a 60A·MeV ^{48}Ca beam on a thin Be target. γ-ray energies, intensities, $\gamma\gamma$ coincidences and γ-ray angular anisotropies have been measured. The level scheme of ^{45}Ar is proposed for the first time, while that of ^{46}Ar has been extended to states above the previously known 2^+ first excited state. An isomeric state at 537 keV of $0.34^{+0.32}_{-0.15}$ ns lifetime has been found in ^{45}Ar from the line-shape analysis of the γ-ray connecting the first excited state to the ground state. The experimental results are interpreted using shell-model calculations.

Key words: fragmentation reaction of ^{48}Ca beam on a Be target, E=60 MeV·A; measured ^{45,46}Ar, ^{39,41,43}S E_γ, I_γ, ^{45,46}Ar γ-ray multiplicity $\gamma\gamma$ coincidence, angular distribution ratios; ^{45,46}Ar deduced levels, J, π; $T_{1/2}$. 3 segmented Ge clover detectors, 74 BaF_2 detectors, SPEG spectrometer with plastic scintillator, ionization and drift chambers. Large scale shell model calculations.

PACS 21.10.Hw, 23.20.Lv, 21.60.Cs, 27.40.+z

1 Introduction

Signatures of shell effects around magic nuclei manifest themselves in even-even nuclei by the observation of a relatively high energy of the first 2^+ excited state and a weak B(E2:$0^+ \rightarrow 2^+$) or of a sudden drop in the binding energies. All of these features are found at all major shell closures. A change in these characteristics may question the presence of shell effects.

One of the first indications of shell-closure weakening at a magic number was the observation of the low energy of the 2^+_1 state in the N=20 nucleus ^{32}Mg [1]. Deviations from the other two requirements were also shown. The increasing amount of information on N=20 nuclei suggest that the erosion of the N=20 shell is connected to anomalous lowering of multi-particle-multi-hole intruder configurations. This results in the development of an island of inversion around ^{31}Na.

[1] present address: INFN-Laboratori Nazionali del Sud, via S.Sofia 44, 95123 Catania, Italy

Recent experimental data suggest a similar erosion also for the $N = 28$ shell in very neutron rich nuclei. Actually, the onset of deformation in some of the $N = 28$ isotones by neutron particle-hole excitations is more natural than that in the N=20 isotones. At $N = 28$, excitations across the shell-gap take place within the same oscillator shell, between orbitals strongly connected by quadrupole interactions. Thus, even a small amount of excitations across $N = 28$ may lead to permanent quadrupole deformation. According to the β-decay [2] and Coulomb-excitation [3] experiments, quadrupole ground-state deformation develops already at $Z = 16$. Study of the neutron-rich $^{40-44}$S using the in-beam γ-spectroscopy technique [4] suggested a deformed ground state for ^{40,42}S and a mixed deformed configuration for ^{44}S in accordance with both the mean field [5–9] and the recent large-scale shell model calculations [10]. The role of proton collectivity contribution by the decrease of the $\pi d_{3/2}$-$\pi s_{1/2}$ energy difference has been pointed out also in refs. [11,12,4].

All these theories suggest that the erosion of the $N = 28$ shell also takes place by lowering of the deformed intruder configurations. A recent finding of an isomeric state in ^{43}S [13] can be interpreted as the first experimental sign showing in this direction. Determination of the energy of the $3/2^-_1$ state in ^{45}Ar and the 0^+_2 state in ^{46}Ar may help to understand how the melting of the $N = 28$ shell gap in neutron rich nuclei takes place.

From the β-decay study of ^{45}Cl, Winger *et al.* [14] has already assigned some γ-rays to ^{45}Ar, while the energy and lifetime of the first 2^+ excited state in ^{46}Ar are known from the Coulomb excitation experiment performed by Scheit *et al.* [15]. From deep inelastic reaction, Fornal *et al.* have obtained a precise energy for this 2^+ state [16].

To obtain further information on the excited states in ^{45,46}Ar we have investigated these nuclei at GANIL, by the in-beam γ-spectroscopy technique using the fragmentation of a ^{48}Ca beam. This method have been proven to be successful to study excited states of exotic nuclei [17,18].

2 Experimental methods

A ^{48}Ca^{20+} beam of 60.3 MeV·A energy and 15 enA intensity was fragmented on a ^{9}Be target of 2.76 mg/cm^2 thickness. The emerging fragments were detected by the SPEG spectrometer whose magnetic rigidity was optimized for the transmission of fully stripped $^{44}_{16}$S nuclei. At this Bρ setting, the $^{45,46}_{18}$Ar^{17+} nuclei were transmitted in their Q=Z-1 charged state within the 7% momentum acceptance of the spectrometer. Ionization and drift chambers, as well as a plastic scintillator were placed at the SPEG focal plane, which provided measurement on the energy loss (ΔE), the total energy (E), and the time-of-flight (t.o.f) for the identification the fragments. The t.o.f of the fragments was corrected according to their path lengths through the spectrograph. The ΔE-E selection was used to distinguish between nuclei of different charge states with similar A/Q values. During the experiment about $1.1{\cdot}10^5$ ^{45}Ar nuclei and $2.7{\cdot}10^5$ ^{46}Ar nuclei were identified.

The fragmentation of the ^{48}Ca beam populates Ar nuclei in different excited states which eventually de-excite by the emission of γ-rays in flight. These γ-rays were detected by 74 BaF_2 and 3 segmented Ge clover detectors which surrounded the Be target. The BaF_2

crystals were mounted symmetrically above and below the target at a mean distance of 16 cm, covering about 80% of the total solid angle. The 3 segmented Ge clover detectors were placed at about 15 cm from the target at the angles of 85°, 122° and 136° with respect to the beam direction. The γ-ray spectra were corrected for the Doppler-shift caused by the large fragment velocity ($v/c = 0.34$). The Doppler broadening due to the finite solid angle of the detectors was decreased by utilizing the electronic segmentation of the clover detectors. After these corrections a full width at a half maximum of about 35 keV was obtained at the γ-ray energy of 1570 keV. The γ rays were identified by use of the high resolution spectra from the Ge detectors, while their coincidence relationships were deduced using the relatively high efficiency of the BaF_2 detectors.

Angular distributions of the strongest γ-transitions were found to be non-isotropic. As the clover detectors were placed at three different angles, we could determine the γ-ray intensity ratios for two pairs of angles. After normalization of these ratios to the 1570 keV stretched E2 transition of ^{46}Ar [15,16] the obtained anisotropy ratios have been found to cluster into two groups. All the known stretched E2 transitions fall within the first group, while the second group was formed by the anisotropy ratios of some transitions known to have a dipole character such as in ^{41}Cl. This difference in the anisotropy ratios suggests that the stretched quadrupole and stretched dipole transitions can be distinguished. We used this possibility to assign the spins of some of the excited states.

3 Experimental results

The γ-ray spectra obtained for ^{45,46}Ar by the use of the Ge clover detectors are shown in Fig. 1. The inserts show the γ-γ coincidence spectra from the BaF_2 detectors obtained by gating on the 1570 keV γ-ray in ^{46}Ar and on the 537 keV γ-ray in ^{45}Ar.

In the case of ^{46}Ar, the strongest 1570(5) keV γ ray was observed both in Coulomb excitation [15] and deep inelastic [16] experiment. The energy of the transition is in a reasonable agreement with the more precise value of 1577(1) keV [16]. In addition to this transition we firmly assign to this nucleus four γ-rays of energies 1919, 2322, 2721 and 3507 keV. As it can be seen in the insert of Fig. 1 an additional transition of 1140 keV energy, which was hidden under the Compton-edge of the 1570 keV γ-line, has been attributed to this nucleus. The 1570 keV γ-ray is by far the most intense, which confirms its assignment to the 2^+ to 0^+ transition in ^{46}Ar [15,16]. The 1140 keV transition is feeding the 1570 keV level according the γ-γ coincidence relationship, resulting in a state at 2710 keV. The sum of the energies of the 1570 keV transition and of the 1919 keV weak γ ray gives the energy of 3489 keV. Within the experimental errors, this value is similar to the weakly observed γ-transition at 3507(16) keV (see Fig. 1). This suggests the existence of a state at 3507 keV. The fact that this level is connected to the first 2^+ and to the 0^+ ground state allows for (1^+,2^+) spin-parity assignment to that state, from which possibilities the 2^+ is more likely. The relative intensity of the 2322 keV γ-ray is higher in the coincidence spectrum with a γ-ray multiplicity condition higher then one, than in the single (multiplicity equal to one) spectrum. It is, therefore, a member of a γ-ray cascade which could originate from a level located at 3892 keV. Finally, the weak

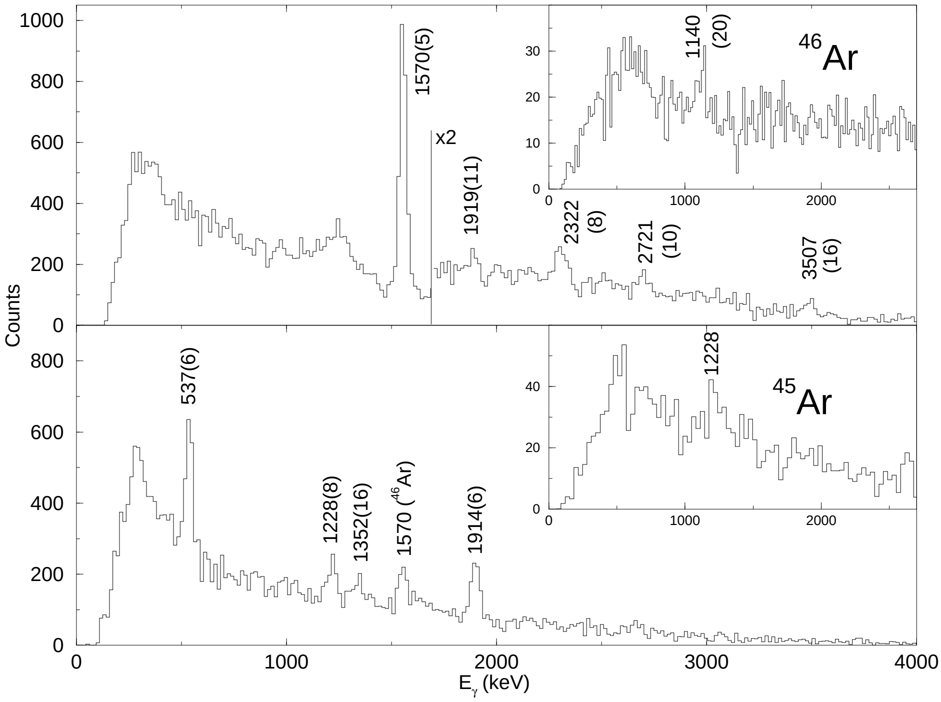

Fig. 1. γ-ray spectra of ^{45,46}Ar obtained by the use of Ge detectors. The spectra shown in the insert have been obtained from the BaF_2 detectors by gating on a 1570 keV (top spectrum) and the 537 keV (bottom spectrum) γ-line.

2721 keV transition was tentatively placed on top of the 1570 keV state.

Angular anisotropy ratios are shown for the 2322 keV γ-ray in ^{46}Ar in Fig. 2. These ratios fall into the region of known E2 transitions. Since the angular distributions of the stretched quadrupoles and of the non-stretched dipoles are similar, we cannot distinguish them. Thus, we conclude that the 2322 keV transition connect states with a spin difference of 2 or $0\hbar$. Keeping in mind that the 1570 keV level has a 2^+ spin, it is surmised that the 3892 keV level would have a $J^\pi = 0, 2, 4^+$ spin value. We could reject the 0 and 2 spin values from the following arguments. In the case of a 0^+ spin, the 2322 keV transition should have an isotropic angular distribution, and the anisotropy ratio should fall between the ΔJ=1 and ΔJ=2 ratios. however, its mean value is centered in the ΔJ=2 zone as shown in fig. 2, which makes the 0^+ spin value for the 3892 keV state unlikely. The non observation of the direct decay of the 3892 keV state to the ground state as expected for a typical 2_2^+ excited state makes the spin 2^+ assignment also unlikely. As deduced from these considerations, the level scheme of the ^{46}Ar nucleus is shown in Fig. 3.

We assign to ^{45}Ar four γ-rays with the energies of 537, 1228, 1352 and 1914 keV among which the 537 keV line is the strongest. The 537 and 1228 keV transitions have already been observed in the β-decay study [14]. From the present work, it is found that these two γ-rays are in coincidence. From γ-ray intensity arguments, it is deduced that the energy of the first excited state is 537 keV and that the 1228 keV γ-ray represents the decay of an excited state at 1765 keV to the first excited state. On the other hand, both the 1914 keV and the 1352 keV γ-rays are not in coincidence with the 537 keV γ-ray which suggests that they are connecting two different excited states to the ground state.

From β-decay studies, spin values of J=3/2 or 5/2 were deduced for the ground state

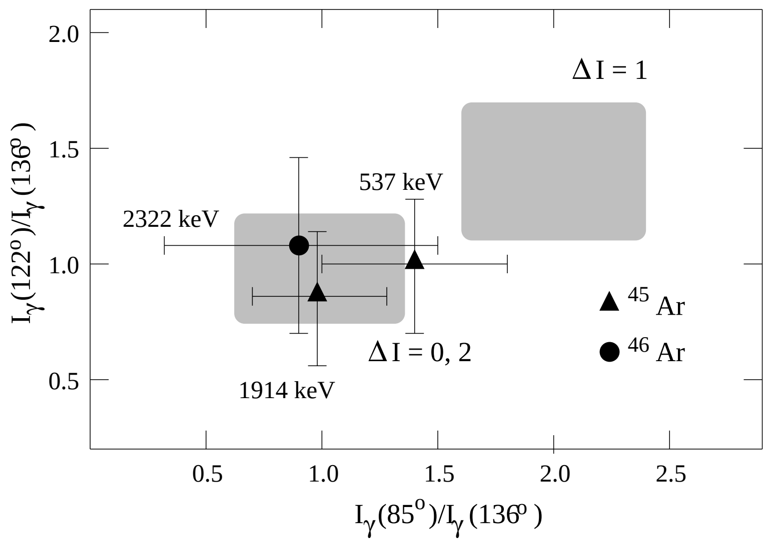

Fig. 2. Anisotropy ratios deduced for the transitions of ^{45,46}Ar. The shaded areas delimit anisotropy ratios for different ΔJ=0,2 or 1 values. They were determined from the strongest γ-ray transitions observed in the experiment.

in ^{43}Ar [19]. By comparing the β branching ratios and the corresponding $\log ft$ values observed in β-decay of ^{43}Ar and ^{45}Ar [19,20], it seems that ^{45}Ar rather decays to states with higher spins than in the case of the decay of ^{43}Ar. These differences in the β branching ratios are consistent with the assumption of J^{π} =$(7/2)^{-}$ for the ground state of ^{45}Ar. This assumption is in agreement with the prediction of the shell model calculations.

Angular anisotropy ratios for the 1914 keV transition fall into the region of known E2 transitions, the ratio for the 537 keV transition lie nearby. Following the same arguments as for ^{46}Ar, we conclude that the 537 and 1914 keV transitions connect states with a spin difference of 2 or $0\hbar$. We could propose the $3/2,7/2,11/2^{-}$ spin-parity values to both states at 537 and 1914 keV. While the 1352 and 1914 keV transitions were not observed in the β decay of ^{45}Cl whose expected ground state spin value is low (J=1/2,3/2), the 537 and 1228 keV transitions were observed in the same β-decay [14]. Thus, the 1914 keV state would have a higher spin value, while the states at 537 and 1228 keV should have some lower spin value. On the basis of this argumentation the 3/2 spin assignment for the 1914 keV state, as well as the possible 7/2,11/2 spin values for the 537 keV state can be discarded. A tentative spin (1/2,3/2) value can be assigned to the 1765 keV state, and a higher (5/2-11/2) spin to the 1352 keV one. As the ground state spin is uncertain, all the assigned spin values are considered to be tentative.

By analyzing the angular distribution of the 537 keV transition, it was found that the γ-line is about twice as wide at 85° than at 135° which is not the case for other lines observed. When emitted from a short-lived excited level of few ps lifetime, the γ-rays are emitted in flight from the target position located at the center of the γ-detector array. We subsequently apply Doppler shift corrections to the energy of the emitted photon according to the angle at which it is detected. In case of a ns-lifetime isomer, the state decays all the way from the target to a few tens of cm downstream the target. Depending

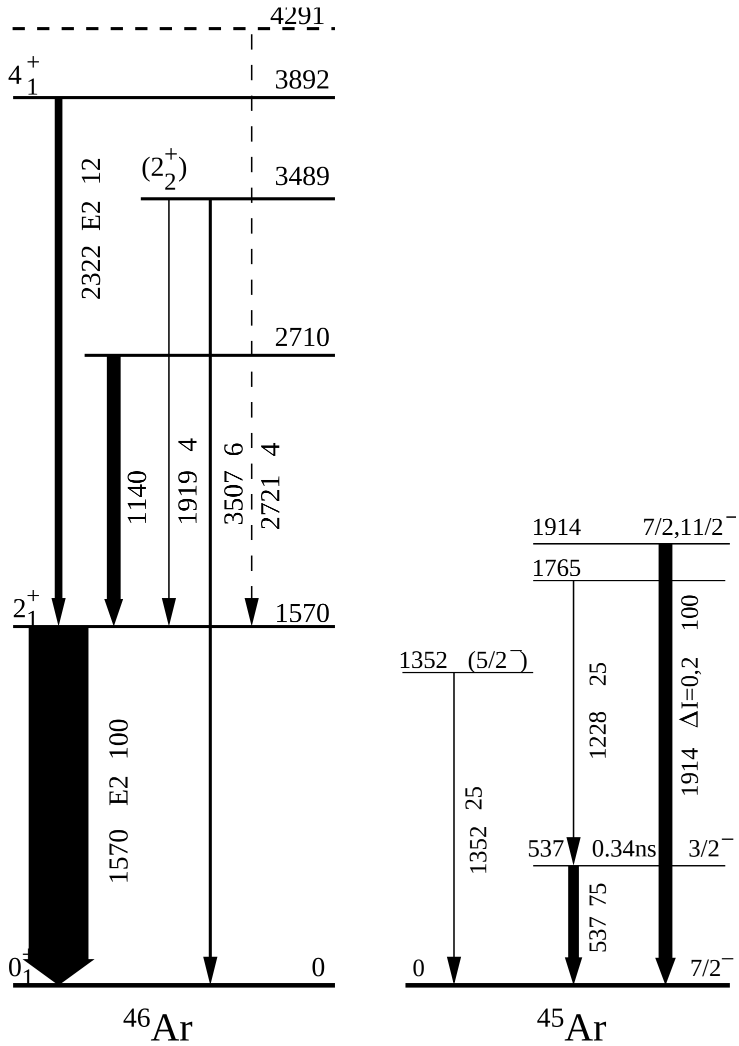

Fig. 3. Proposed level schemes of ^{45,46}Ar from the present experiment. Along the γ-transitions their energies (with uncertainties), multipolarities and relative intensities are given.

on where the γ-ray is emitted the detectors see it with different angles. This of course introduces an additional uncertainty which results in an additional Doppler broadening. By comparing the line width of the γ-peak with those simulated by assuming different half lives, we could deduce a half life of $0.34^{+0.32}_{-0.15}$ ns for the 537 keV state in ^{45}Ar as shown in fig.4. This half-life value fits with a single-particle E2 transition, which confirms the $3/2^-$ spin assignment of the state at 537 keV.

As a byproduct of this investigation we have obtained the γ spectra also of the odd ^{39,41,43}S isotopes, with very low statistics, which allowed only for identification of a few transitions in these nuclei. Namely, we observed the γ ray with 904(7) keV energy in ^{39}S, with 451(3), 1120(14) and 1629(9) keV in ^{41}S and with 1549(9) keV energy in ^{43}S in addition to the known 940 keV transition.

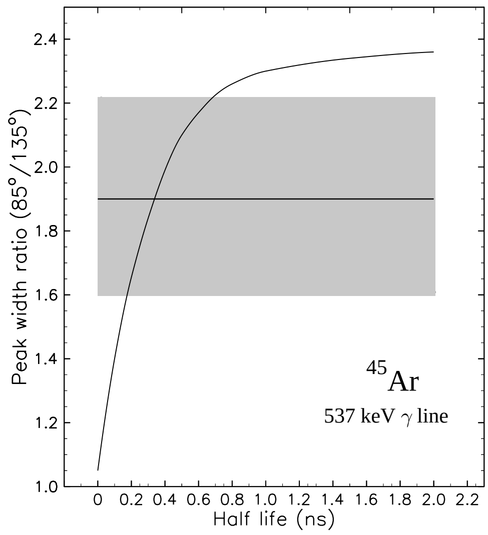

Fig. 4. Comparison of the peak width ratio obtained for the 537 keV transition of ^{45}Ar at 89° and 136° experimentally (horizontal line with the hatched zone representing its uncertainty) with that obtained from a GEANT simulation assuming different half lives (solid curve).

4 Discussion

Prior to the present experiment, the 2^+ energy and the B(E2) of ^{46}Ar were already known [15]. From these data it was deduced by Scheit et al. that ^{46}Ar could be considered as a vibrational nucleus [15]. According to mean-field calculations performed both in relativistic Hartree-Bogolyubov [9] and Hartree-Fock-Bogolyubov [7,8] approximations, the N=28 ^{46}Ar nucleus exhibits a flat potential energy surface centered at a slightly oblate shape. It is likely that vibration occurs around such shape. Starting with the potential energy obtained from mean field calculation, the energy spectrum of ^{46}Ar was calculated by using the angular momentum projected generator coordinate method (GCM) [8]. This model predicts the states 2_1^+, 0_2^+ and 4^+ states at respectively 1.8 MeV, 2.8 MeV and 4.5 MeV. The 0_2^+ energy is close to the level observed experimentally at 2.71 MeV. Other excited states are slightly higher than the measured ones. This could be due to the fact that the calculation neglects the angular-velocity dependence of the moment of inertia. This dependence has been shown to amount to about 13% for 2_1^+ and 4^+ in the HFB calculations of ^{44}S [4]. Applying a similar reduction to the moment of inertia makes the yrast sequence closer to experiment in ^{46}Ar.

Shell model calculations have been performed for ^{45,46}Ar using the interaction given in Ref. [21]. Calculations are compared with the experimental results in Fig. 5. All the levels deduced experimentally have a theoretical counterpart in ^{46}Ar. Similar agreement is found up to 2 MeV in ^{45}Ar with the exception of one state which is not observed experimentally. The calculated quadrupole moment of the 2_1^+ state in ^{46}Ar is positive [10]. This corresponds to excitation of an oblate nucleus, which agrees with the mean field calculations.

In order to analyze, how the N = 28 shell closure persists in ^{46}Ar, we extract the *0p0h*

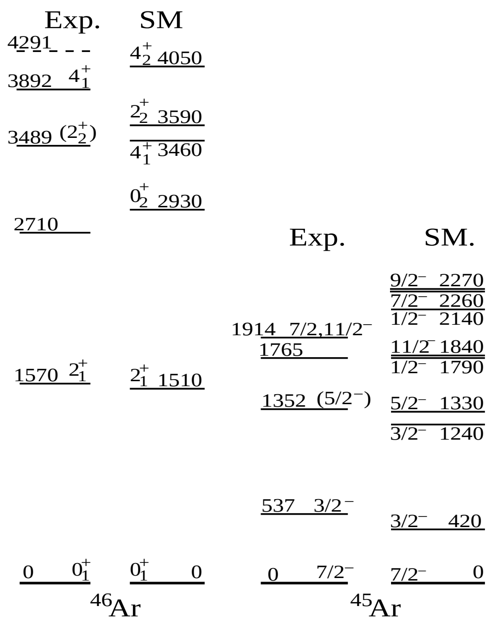

Fig. 5. Comparison of the experimental level schemes of ^{45,46}Ar with those obtained from large scale shell model calculations.

and *2p2h* neutron components of the 0^+ eigenstates of ^{46}Ar using the Lanczos Structure Function method of ref [22]. This shows that the normal *0p0h* configuration strongly dominates the ground state configuration with the *2p2h* components being mainly located in the second and third excited states. Thus, the shell model calculations suggest an intruder configuration for the experimental state at 2.71 MeV, in accordance with the results of the GCM calculations. The contribution of the intruder configurations to the ground state wave function becomes significant in ^{44}S as a result of a further decrease in the $N = 28$ gap energy [4].

As just discussed from the shell model point of view, the ^{46}Ar ground state has a pure *0p0h* neutron configuration with respect to ^{48}Ca. However, two effects could simultaneously favor *2p2h* excitations. First, calculations predict that the $N = 28$ gap between the $p_{3/2}$ and $f_{7/2}$ orbitals is progressively reduced when removing protons from ^{48}Ca (4.73 MeV in ^{48}Ca, 3.84 MeV in ^{46}Ar) therefore the neutron excitations across the gap cost less energy. Second, the energy of the cross shell excitations is further reduced by an energy gain obtained from the additional correlation between the protons and the newly generated 2 neutron particles and holes. The strength of the correlation energy is increasing towards mid-shell, it is calculated to be 4.08 MeV in ^{48}Ca and 5.98 MeV in ^{46}Ar. These values reduce the net cost required to promote 2 neutrons in the $p_{3/2}$ shell. The emergence of an intruder g.s. configuration would be found when this gain in correlation energy is larger than the cross shell excitation. This feature eventually brings deformation to the nuclei.

According to the shell model, the N=27 isotones also reflect a regular transition from sphericity to deformation in their low-lying spectrum. It is the excitation energy of the $\frac{3}{2}^-$ state which should be sensitive to the correlations and also to the N=28 neutron gap. The systematics of the energy of the $3/2_1^-$ states relative to the $7/2^-$ ones in N=27 nuclei is shown in Fig. 6. The $3/2_1^-$ state lies at around 2 MeV in ^{47}Ca, and decreases gradually from each side of Z=20. Its excitation energy arises from its structure, which is

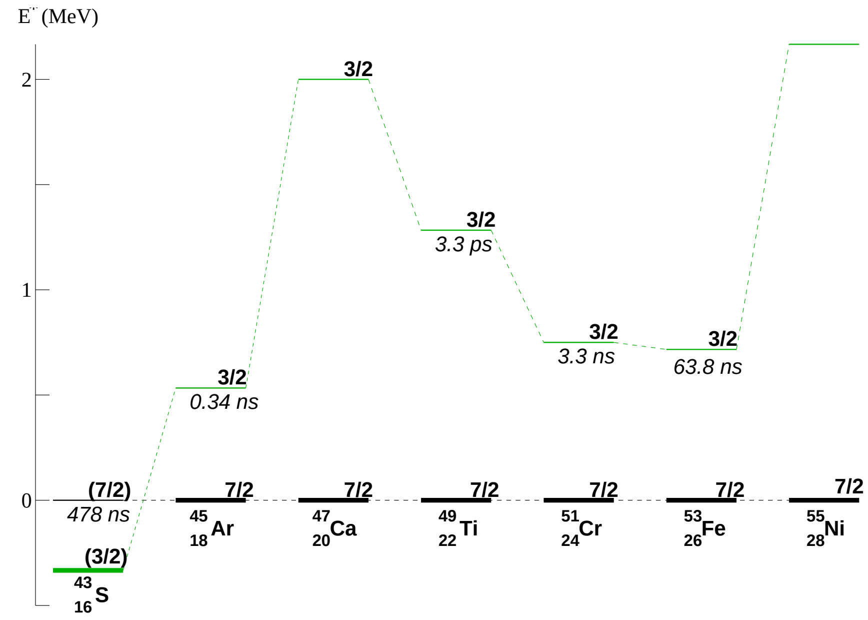

Fig. 6. Comparison of the experimental energies of the $7/2^-$ and $3/2^-$ states in N=27 nuclei.

a mixture of particle-hole excitation across the gap mainly to the $p_{3/2}$ state and coupling of the neutron hole to the 2^+ proton state. One can get information on the strength of the mixing from the life time of the $3/2^-$ state. When its configuration is mainly of intruder origin, are strongly retarded, as it can be seen in the case of ^{51}Cr and to a larger extent in ^{53}Fe [23]. Although, the half life of the first $3/2^-$ state in ^{45}Ar is relatively long, after correcting for the energy scaling factor of E_γ^5, it has a rather weak retardation compared to ^{53}Fe. The ∼1 Weisskopf unit experimental E2 strength corresponds to the situation in ^{49}Sc and agrees well with shell model predicting only a small intruder admixture. According to the Lanczos Structure Function method, the first $3/2^-$ state collects about 15% 1p2h component, while most of the intruder strength is concentrated in the second $3/2^-$ state at 1.2 MeV, which was experimentally not observed. The retardation of the E2 transition in ^{43}S is similar to that observed in ^{51}Cr and is well described by the shell-model calculations predicting a strong mixing between the intruder and normal configurations [21].

5 Conclusion

Using a novel technique based on the in-beam γ-spectroscopy used with fragmentation reactions at intermediate energy, the level schemes of ^{46}Ar has been extended to higher excitation energy and higher spin and a level scheme of ^{45}Ar has been suggested for the first time. These results represent the missing link between the N=27,28 Ca and S nuclei, making possible the systematic study of changes in their structure. The sudden lowering of the energy of the first $3/2^-$ state in ^{45}Ar gives additional credit to the believe that it may become the ground state in ^{43}S [13] in agreement with the shell model prediction. The way how ground state deformation develops in the N=28 isotones could be traced back from the 0_2^+ states in even nuclei. In ^{46}Ar, the 0_2^+ state at about 2.7 MeV is expected to have a 2p2h configuration. In ^{44}S, the unperturbed energy of the $0_1^+, 2$ states becomes nearly degenerate resulting in strongly mixed 0^+ states in ^{44}S [4].

According to theoretical models and experimental findings, the size of the $N = 28$ shell gap seems to be reduced south to ^{48}Ca. This may give rise to a new island of inversion at low-Z, $N = 28$ nuclei. Whether it is the case does depend on the correlation energy too. Its value would be reduced if a strong Z=14 sub-shell closure exists. The structure of neutron-rich $_{14}$Si isotopes around $N = 28$ has to be explored in order to clarify the situation about the $N = 28$ reduction and the emergence of a new island of inversion.

Acknowledgments The experiment using in-beam gamma spectroscopy with fragmentation reactions benefit from the availability of ^{48}Ca isotope kindly provided by our colleagues from DUBNA and from the smooth running of the accelerator by the GANIL crew. The use of the segmented clover detectors was made possible thanks to the EXOGAM Collaboration. This work has been supported by the European Community contract N° HPRI-CT-1999-00019, by OTKA D34587,T30497, and Bólyai János Foundation.

References

[1] D. Guillemaud-Mueller, C. Detraz, M. Langevin, F. Naulin, M.De Saint-Simon, C. Thibault, F. Touchard, M. Epherre, Nucl. Phys. **A426** (1984) 37.

[2] O. Sorlin, D. Guillemaud-Mueller, A.C. Mueller, V. Borrel, S. Dogny, F. Pougheon, K.-L. Kratz, H. Gabelmann, B. Pfeiffer, A. Wöhr, W. Ziegert, Yu.-E. Penionzhkevich, S.M. Lukyanov, V.S. Salamatin, R. Anne, C. Borcea, L.K. Fifield, M. Lewitowicz, M.G. Saint-Laurent, D. Bazin, C. Détraz, F.-K. Thielemann, W. Hillebrandt, Phys. Rev. C **47** (1993) 2941.

[3] T. Glasmacher, B.A. Brown, M.J. Chromik, P.D. Cottle, M. Fauerbach, R.W. Ibbotson, K.W. Kemper, D.J. Morrissey, H. Scheit, D.W. Sklenicka, and M. Steiner, Phys. Lett. B**395** (1997) 163.

[4] D. Sohler, Zs. Dombrádi, J. Timár, O. Sorlin, F. Azaiez, F. Amorini, M. Belleguic, C. Bourgeois, C. Donzaud, J. Duprat, D. Guillemaud-Mueller, F. Ibrahim, J.A. Scarpaci, M. Stanoiu, M.J. Lopez, M.G. Saint-Laurent, F. Becker, F. Sarazin, C. Stodel, G. Voltolini, S.M. Lukyanov, V. Maslov, Yu.-E. Penionzhkevich, M. Girod, S. Peru, F. Nowacki, G. Sletten, R. Lucas, C. Theisen, D. Baiborodin, Z. Dlouhy, J. Mrazek, C. Borcea, A. Bauchet, C.J. Moore, M.J. Taylor, Phys. Rev. C **66** (2002) 054302.

[5] T.R. Werner, J.A. Sheikh, M. Misa, W. Nazarewicz, J. Rikowska, K. Heeger, A.S. Umar, M.R. Strayer, Nucl. Phys. **A597** (1996) 327.

[6] P.-G. Reinhardt, D.J. Dean, W. Nazarewicz, J. Dobaczewski, J.A. Maruhn, and M.R. Strayer, Phys. Rev. C **60** (1999) 014316.

[7] S. Péru, M. Girod, and J.F. Berger, Eur. Phys. J. A**9** (2000) 35.

[8] R. Rodriguez-Guzman, J.L. Egido, L.M. Robledo, Phys. Rev. C **65**, (2002) 024304.

[9] G.A. Lalasissis, D. Vretenar, P. Ring, M. Stoitsov, and L.M. Robledo, Phys. Rev. C **60** (1999) 014310.

[10] E. Caurier, F. Nowacki, and A. Poves, Eur. Phys. J. A**15**, 145 (2002)

[11] J. Retamosa, E. Caurier, F. Nowacki, and A. Poves, Phys. Rev. C **55** (1997) 1266.

[12] P.D. Cottle, and K.W. Kemper, Phys. Rev. C **58** (1998) 3761, and Phys. Rev. C **66** (2002) 061301.

[13] F. Sarazin, H. Savajols, W. Mittig, F. Nowacki, N.A. Orr, Z. Ren, P. Roussel-Chomaz, G. Auger, D. Baiborodin, A.V. Belozyorov, C. Borcea, E. Caurier, Z. Dlouhy, A. Gillibert, A.S. Lalleman, M. Lewitowicz, S.M. Lukyanov, F. De Oliveira, Y.E. Penionzhkevich, D. Ridikas, H. Sakurai, O. Tarasov, A. de Vismes, Phys. Rev. Lett. **84** (2000) 5062.

[14] J.A. Winger, H.H. Yousif, W.C. Ma, V. Ravikumar, W. Lui, S.K. Phillips, R.B. Piercy, P.F. Mantica, B. Pritychenko, R.M. Ronningen, and M. Steiner, AIP Conf. Proc. **455** (1998) 606.

[15] H. Scheit, T. Glasmacher, B.A. Brown, J.A. Brown, P.D. Cottle, P.G. Hansen, R. Harkewicz, M. Hellström, R.W. Ibbotson, J.K. Jewell, K.W. Kemper, D.J. Morrisey, M. Steiner, P. Thirolf, and M. Thoennessen, Phys. Rev. Lett. **77** (1996) 3967.

[16] B. Fornal, R. Broda, W. Królas, T. Pawlat, J. Wrzesiński, D. Bazacco, S. Lunardi, C. Rossi Alvarez, G. Viesti, G. de Angelis, M. Cinausero, D. Napoli, J. Gerl, E. Caurier, F. Nowacki, Eur. Phys. J. A **7** (2000) 147.

[17] M.-J. Lopez-Jimenez, PhD Thesis, GANIL T 00 01, GANIL, Caen, 2000, and M.-J. Lopez-Jimenez, *Int. Winter Meeting On Nuclear Physics*, Bormio 1999, Ricerca Scientifica et Educazione Permanente Supplemento 114 (1999) 416.

[18] M. Belleguic-Pigeard de Gurbert, PhD thesis, IPNO-T-00-05 Institute de Physique Nucleaire, Orsay, 2000, and M. Belleguic *et al.*, Phys. Scripta T**88** (2000) 122.

[19] J.A. Cameron, B. Singh, Nucl. Data Sheets **92** (2001) 783.

[20] T.W. Burrows, Nucl. Data Sheets **65** (1992) 1.

[21] S. Nummela, P. Baumann, E. Caurier, P. Dessagne, A. Jokinen, A. Knipper, G. Le Scornet, C. Miehe, F. Nowacki, M. Oinonen, Z. Radivojevic, M. Ramdhane, G. Walter, J. Aysto, and the ISOLDE Collaboration, Phys. Rev. C **63** (2001) 044316.

[22] F. Nowacki, Nucl. Phys. **A704**, 223c (2001).

[23] J.L. Wood, K. Heyde, W. Nazarewicz, M. Huyse and P. van Duppen, Phys. Rep. **215** (1992) 101.